

Purdue University
Purdue e-Pubs

International Compressor Engineering Conference

School of Mechanical Engineering

2000

Vibration-Acoustics Study of R410A Rotary Compressors

W. Zhou

United Technology Carrier Corporation

M. Daniels

United Technology Carrier Corporation

I. Hwang

Daewoo Carrier Corporation

C. Kim

Daewoo Carrier Corporation

K. Yun

Daewoo Carrier Corporation

Follow this and additional works at: <https://docs.lib.purdue.edu/icec>

Zhou, W.; Daniels, M.; Hwang, I.; Kim, C.; and Yun, K., "Vibration-Acoustics Study of R410A Rotary Compressors" (2000).
International Compressor Engineering Conference. Paper 1497.
<https://docs.lib.purdue.edu/icec/1497>

This document has been made available through Purdue e-Pubs, a service of the Purdue University Libraries. Please contact epubs@purdue.edu for additional information.

Complete proceedings may be acquired in print and on CD-ROM directly from the Ray W. Herrick Laboratories at <https://engineering.purdue.edu/Herrick/Events/orderlit.html>

VIBRATION- ACOUSTICS STUDY OF R410A ROTARY COMPRESSORS

Wei Zhou and Mark Daniels
Aeroacoustics and Vibration Research, Corporate Technology
United Technology Carrier Corporation
Carrier Parkway, P.O. Box 4808, Syracuse, NY 13221, USA

Insoo Hwang, Chulwon Kim and Kyungwoo Yun
Rotary Compressor Engineering, Daewoo Carrier Corporation
981-11 Jangduk-dong, Kwangsan-gu, Kwangju, Korea

ABSTRACT

This paper demonstrates a typical process to investigate the vibro-acoustic behavior of R410A rotary compressors. The compressor shell is usually the main noise radiator in a rotary compressor. However, the accumulator shell can be a significant noise source as well, although its size is relatively small. Sound performance of a rotary compressor is affected not only by the dynamic characteristics of the compressor and accumulator shells, but also by the baseplate and connecting structures between the accumulator and compressor shell (e.g. bracket, strap and suction pipe). The influence of the baseplate and the connecting structures can be significant at low frequencies because rigid-body vibration dominates the motions of the compressor and accumulator shells.

INTRODUCTION

The planned phase-out of environmentally unfriendly chlorine-based refrigerant has led the air conditioning industry to seek an alternative to R22. An alternative *green* refrigerant, R410A appears to be a refrigerant of choice due to its attractive flow and thermal features. However, due to the large relative increase in required operating pressures, R410a compressors tend to be louder than those using R22. For example, at similar operating conditions and for a given capacity, R410A compressors are typically 2 to 3 dB louder than R22 compressors. Figure 1, shows the comparison of sound pressure levels in 1/3-octave-bands for R22 and R410a compressors operating at ARI condition (45/130/65F). An obvious difference is the large increase in the 1,600 Hz band, which is a primary contributor to the overall noise of R410A compressors although a secondary influence on the overall noise of R22 compressors.

A challenge facing compressor and system designers using R410A is that operating pressures and gas densities are significantly higher thereby requiring special needs from both system design and noise abatement viewpoints. A comparison of R22 and R410A refrigerants is shown in Table 1 for saturated gas properties at ARI condition. The working gas pressures and densities in R410A compressors are much higher than those in R22 compressors, however the speeds of sound are very close to each other at both suction and discharge conditions. Compressor internal forces, including bearing forces, gas pulsation forces and valve-impact forces, directly contribute to the radiated noise.

High operating pressures and gas densities in R410A compressors will cause significant increases in these internal forces. This helps explain why R410A compressors are noisier. However, to be effective at reducing noise in R410A compressors a comprehensive understanding on the vibro-acoustic characteristics of individual compressors needs to be undertaken.

Gas Property		R22	R410A
Pressure (psia)	Suction	90.76	144.5
	Discharge	311.6	490.1
Gas Density (lbm/ft ³)	Suction	1.656	2.391
	Discharge	6.024	10.13
Speed of Sound (ft/sec)	Suction	534.4	551.5
	Discharge	493.9	466.8

Table 1. Comparison of saturated gas properties between R22 and R410A at ARI condition.

INVESTIGATION

This study will investigate how the noise radiated by a R410A compressor is affected by its structural dynamics. In addition, it will include proposed structural design changes for reducing noise.

The diagnosis of the noise problem is a crucial process in a noise reduction procedure. As previously stated, the compressor shell is usually the main noise radiator in a rotary compressor. The accumulator shell can be a significant noise source as well, however its size is usually small in relation to the compressor body. Noise radiated by a rotary compressor is not only affected by the dynamic characteristics of the compressor and accumulator shells, but also by the baseplate and connecting structures between the accumulator and compressor shells (e.g. bracket, strap and suction pipe). The influence of the baseplate and the connecting structures (i.e. their relative stiffness) can be significant at low frequencies because rigid-body motions dominate the movement of compressor and accumulator shells.

Sound and vibration tests were carried out on a selected R410A compressor. The selected compressor had a nominal capacity 9,500 Btu/h and its motor running speed was about 3,000 rpm. The tests were conducted in the full anechoic sound room with *Mobil68* lubrication oil charged in the system. The compressor was mounted using standard grommets on a *rigid* base in a fully anechoic sound room. Structural dynamic analyses were performed using the finite element method on a simplified structural model of the compressor.

Sound Pressure and Power Measurement

The compressor sound pressures and sound powers were measured at several different conditions to identify peak-noise frequencies and their associating compressor components. Figure 2, shows the narrow-band spectrum of the averaged sound pressure level at 5 feet from the compressor center with the compressor operating at ARI condition. As shown special attention must be given to the compressor's structural dynamic characteristics in the frequency band from 1,680 to 1,780 Hz as it appears a structural resonance may be causing a degree of amplification in noise. The 1/3-octave-band sound power and A-weighted spectra are shown in Figure 3. In Figure 3, the noise at 1,600 Hz is at least 2dB higher than that in other bands.

To investigate the influence of the amount of lubrication-oil charge on the compressor sound performance, sound tests were also carried out when the charge was reduced to about two thirds the normal amount. For the convenience and in discussion hereafter, Condition 1 will refer to a compressor with the normal charge (tests results of Figures 2 and 3) and Condition 2 will refer to tests conducted with a reduced oil charge (66% less). Figure 4, shows the narrow band spectrum of the averaged sound pressure measured 5 feet from the compressor center at Condition 2. The overall sound power measured at Condition 2 is about 4dB higher when compared with Condition 1. In addition, by comparing Figure 4 with Figure 2, the following generalities are observed:

- Noise levels in the frequency band from 1,680 Hz and 1,780 Hz at Condition 2 increases significantly.
- The highest peak in the sound pressure spectrum shifts to 1,775 Hz from 1,725 Hz.
- There is no substantial difference among the two sound pressure spectra at other frequencies.

For the compressor tested, reduction of oil charge has negative effects on sound performance and particularly for frequencies from 1,680 Hz to 1,780 Hz. The discussion of actual causes is beyond the scope of the current investigation.

Sound power levels are also measured when the compressor was wrapped with the sound shield and operating at Condition 2. The sound shield consisted of ¾ inch foam with a 1 lbm/ft² barrier. Figure 5 shows the comparison of the sound power levels in the 1/3-octave band measured when the compressor is lagged using two different schemes:

1. Compressor shell unwrapped and accumulator shell wrapped,
2. Compressor shell wrapped and accumulator shell unwrapped.

The 1/3-octave-band sound power without using the sound shield is shown in Figure 5 as well. The figure shows that wrapping the compressor shell attenuates the overall sound more efficiently than wrapping the accumulator shell. Primary benefits from the sound shield occur at frequencies above 630 Hz. At 1,600 Hz and 2,000 Hz, both wrapping schemes provide significant attenuation. The calculated combined sound power levels, measured with only the compressor shell wrapped, and only the accumulator shell wrapped, does not agree with that power measured from the bare (unwrapped)

compressor, especially between 1700 and 1800 Hz. One of the reasons to explain this phenomenon is that the compressor did not operate under the same condition. It may be also explained through the lagging schemes used in the measurement. The sound shield in both lagging schemes may introduce additional mass or damping to the connecting structures. This added mass or damping may significantly impact the dynamic response of the connecting structures. For example unwrapped components such as the accumulator shell, may respond differently when the compressor is wrapped or unwrapped due to reductions in transmitted energy for the wrapped case. Additionally, this phenomenon may indicate that noise radiated between 1,700 to 1,800 Hz is related to the vibration of the connecting structures.

Sound Intensity Measurement

Narrow band (25 Hz bandwidth) sound intensities over the surface of the compressor shell and the accumulator shell were measured. Contour plots at noise-dominant frequencies were generated to discover how noise radiates from each component. In all these cases, the compressor was operating at Condition 2. The intensity on the compressor shell was measured when the accumulator shell was wrapped as in the sound power measurement, and vice versa. This procedure was used to minimize the mutual influences between major acoustic sources, in the frequency range of interest. Partial side surfaces were scanned using a point-to-point intensity mapping method.

Figure 6 shows intensity contours over the compressor shell and the accumulator shell at 1,775 Hz, which is the dominant frequency in the sound pressure spectrum as shown in Figure 4. At this frequency, the highest intensity on the accumulator shell is about 10 dB higher than that on the compressor shell. Sound power levels radiated from the accumulator shell at 1,600 Hz and 2,000 Hz (1/3 octave bands) are nearly the same as those from the compressor shell, as shown in Figure 5. This is consistent with intensity measurements since the surface area of the accumulator shell is much smaller than that of the compressor shell. The peak intensity region of the accumulator shell corresponds to the outside surface that is away from the compressor shell. High intensity regions on the compressor's lower shell are in areas between welding spots. This phenomenon was observed at other frequencies and is consistent with the vibration measurement being discussed in the next section.

Vibration Measurement Using LDV

Compressor vibration was measured by employing a laser Doppler vibrometer (LDV) and vibration motions were animated for visualization at noise-dominant frequencies. The LDV measures the velocity distribution on a vibrating surface with a high spatial resolution. A laser beam from the LDV is focused on a measurement point and the instantaneous velocity of the surface at that point is determined using the Doppler effect. The LDV area scans, consisting of measurement points on the compressor shell and accumulator shell, are shown in Figure 7. An accelerometer mounted on the compressor shell provided a reference signal.

A snap shot of the animated vibration motion at 1,775 Hz is shown in Figure 8 when the compressor operated at Condition 1. It should be noted that the compressor rigid-body motion, which is not insignificant at this frequency, could not be visualized in the figure.

On top of the rigid-body motion, are considerable local deformations on the compressor's lower shell, as shown by the picture on the right in Figure 8. The local deformation of the accumulator shell, as shown by the picture on the left in Figure 8, is associated with the motion of the strap used to hold the accumulator. The significance of these local deformations on noise, in the frequency range from 1,700 to 1,800 Hz, needs further investigation. In general, almost no deformation occurred in regions at and near welding spots and local deformation was observed at frequencies as low as 1,000 Hz.

The natural frequency of the first shell mode was above 4,000 Hz, which was estimated using the finite element method and is discussed in the next section.

Modal Analysis Using FEM

The finite element method (FEM) was used to predict the modal parameters of the compressor. For simplicity the whole compressor is divided into two separate components: the accumulator shell and the compressor shell. The analysis results for the accumulator shell have been reported in References 1. The natural frequency of first shell mode is reported above 3,000 Hz for 81-mm (diameter) steel accumulators.

The finite element model of the simplified compressor shell is comprised of the models for the baseplate, the lower shell, the upper shell and the motor stator. The substructures are connected by sharing common nodes on their interfaces. The finite element model and the first two shell modes are shown in Figure 9. The natural frequencies of the shell modes are estimated above 4,000 Hz. Inclusion of the crankcase and the lubrication oil in the oil sump will change the predicted natural frequencies, but it is believed that the variations would not be significant. Comparing the vibration responses in Figure 8, with the mode shapes in Figure 9, indicates that the breathing mode is excited at relatively low frequencies.

CONCLUSION

Vibration-acoustic performance of a R410A rotary compressor has been studied by measuring its sound power, intensity and structural vibration as well as predicting its modal parameters using the FEM. The dominant noise is in the frequency range from 1,700 to 1,800 Hz, depends primarily on the initial oil-charge amount. The noise level becomes significantly higher if considerably less oil is charged. The highest sound intensity levels at the dominant noise frequency are found on the accumulator shell. The connecting structures potentially play an important role in the transmission and radiation of noise. These sources and structure modifications will be studied in greater detail, in follow-on investigations.

REFERENCE

1. W. Zhou; H.-J. Kim and J. Kim 1998 *Numerical Prediction of Radiated Noise Level from Suction Accumulators of Rotary Compressors*. Proceedings of the 1998 International Compressor Engineering Conference at Purdue.

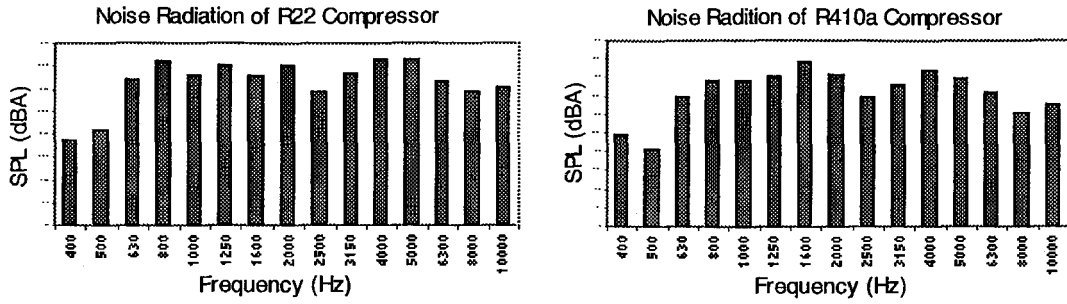


Figure 1. Comparison of 1/3-octave-band sound pressure levels between R22 and R410A compressors (ARI condition).

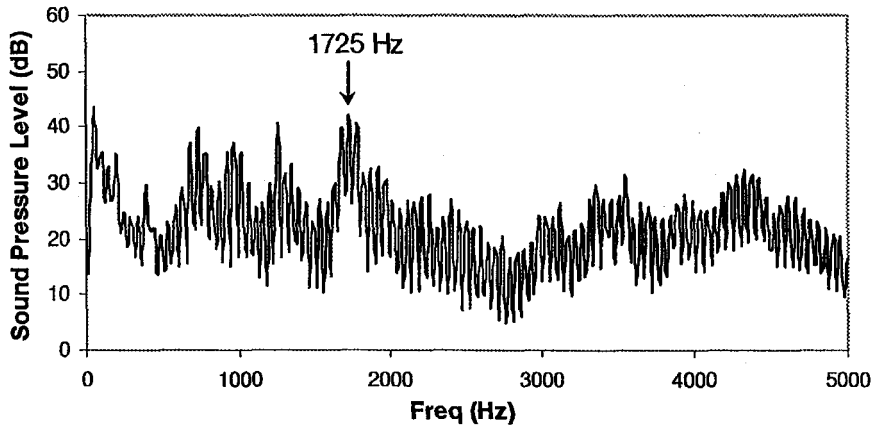


Figure 2. Averaged sound pressure at 5 ft (Narrow Band)

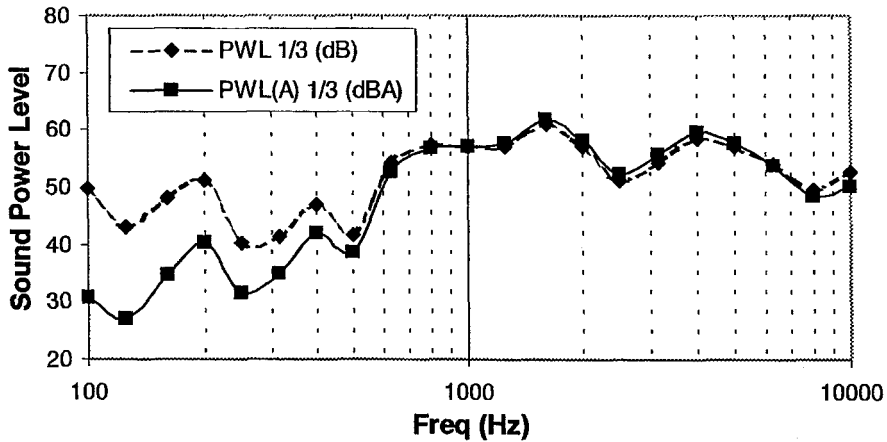


Figure 3. Sound power (1/3 Octave Band)

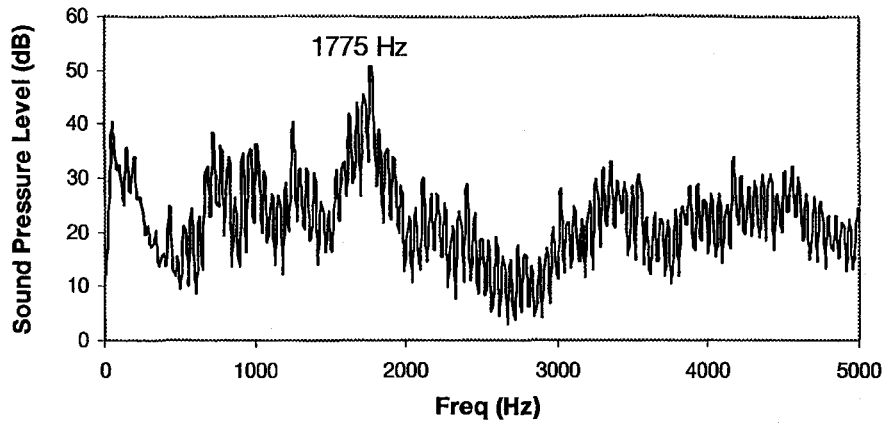


Figure 4. Average sound pressure (Narrow Band) with low oil charge

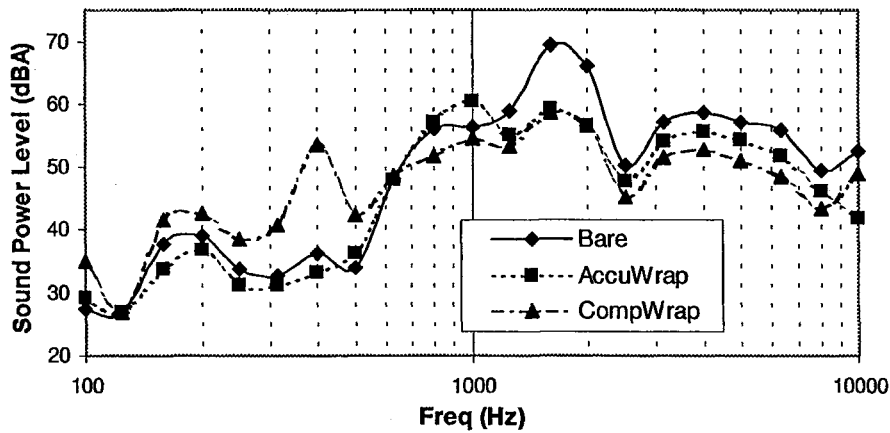


Figure 5. Comparison of sound powers using different lagging schemes
 Bare – No sound shield used; AccuWrap – Compressor unwrapped and accumulator wrapped; CompWrap – Compressor wrapped and accumulator unwrapped.

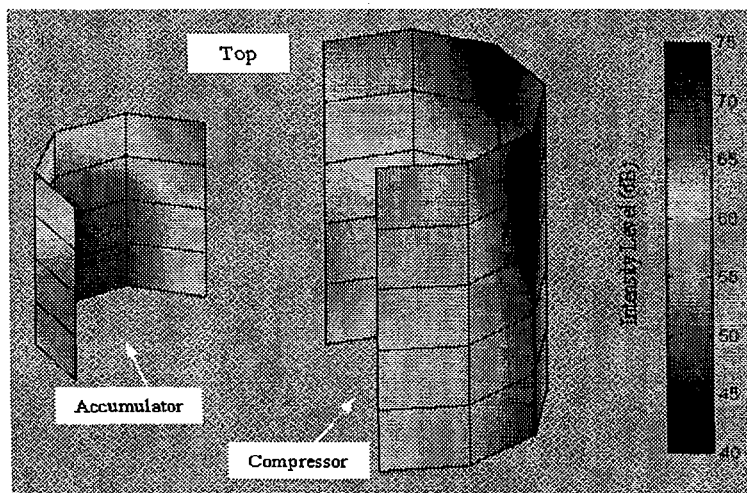


Figure 6. Intensity contours of the compressor and accumulator shells (1775 Hz)

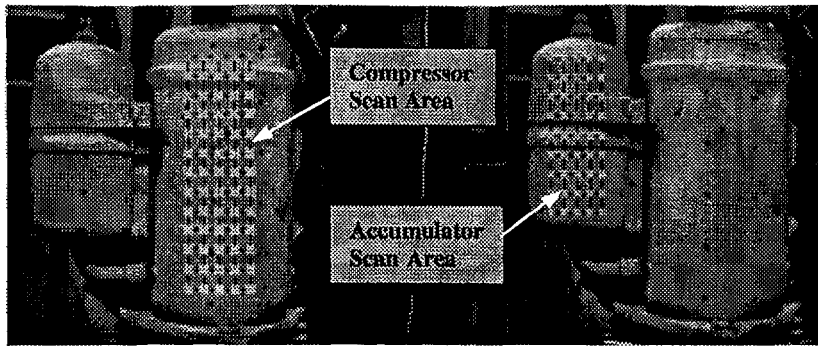


Figure 7. LDV scan areas on the compressor and accumulator shells

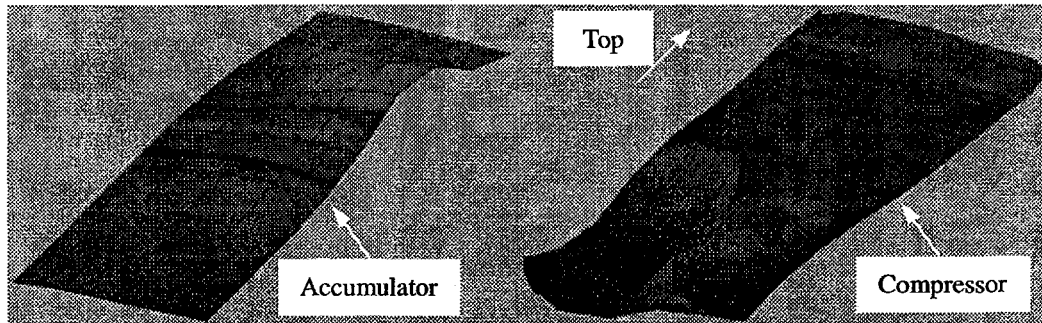


Figure 8. Animated vibration motion of the compressor at 1775 Hz

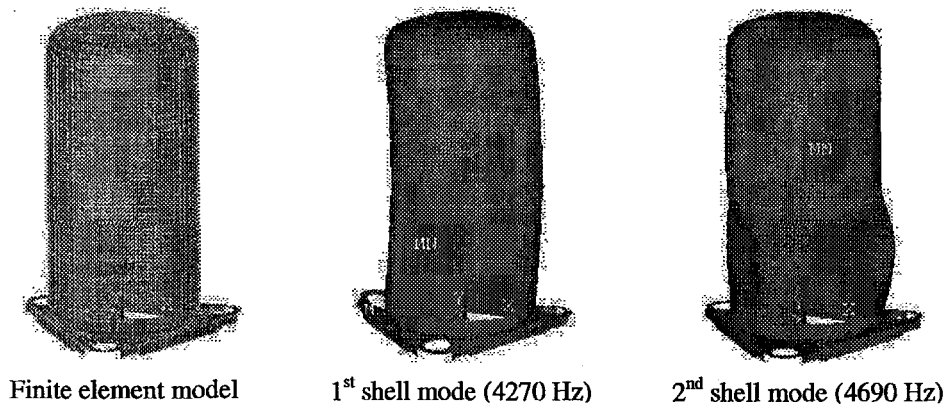


Figure 9. Finite element model and mode shapes of compressor shell